

Beyond Predictive Uncertainty: Reliable Representation Learning with Structural Constraints

Yiyao Yang

yy3555@tc.columbia.edu

ORCID: 0009-0001-8693-4888

Columbia University, New York, NY, United States

Preprint: <https://doi.org/10.4161/748550/arXiv.2601>

I. Abstract

Uncertainty estimation in machine learning has traditionally focused on the prediction stage, aiming to quantify confidence in model outputs while treating learned representations as deterministic and reliable by default. In this work, we challenge this implicit assumption and argue that reliability should be regarded as a first-class property of learned representations themselves. We propose a principled framework for reliable representation learning that explicitly models representation-level uncertainty and leverages structural constraints as inductive biases to regularize the space of feasible representations. Our approach introduces uncertainty-aware regularization directly in the representation space, encouraging representations that are not only predictive but also stable, well-calibrated, and robust to noise and structural perturbations. Structural constraints, such as sparsity, relational structure, or feature-group dependencies, are incorporated to define meaningful geometry and reduce spurious variability in learned representations, without assuming fully correct or noise-free structure. Importantly, the proposed framework is independent of specific model architectures and can be integrated with a wide range of representation learning methods.

II. Literature Review

Most uncertainty quantification in deep learning focuses on predictive uncertainty at the output level, commonly via approximate Bayesian approaches such as MC Dropout (Gal & Ghahramani, 2016), ensemble-based methods (Lakshminarayanan et al., 2017), and post-hoc calibration techniques that adjust predicted probabilities without changing the learned representation (Gul et al., 2017). While these methods improve confidence estimates for predictions, they typically treat intermediate representations as deterministic artifacts and do not explicitly characterize or regularize representation-level reliability. A separate line of work studies representation learning under structural constraints, where geometric or relational inductive biases are imposed to exploit data geometry and improve generalization, such as graph-based or manifold-based regularization (Belkin et al., 2026) and more recent graph-based encoders for structured feature space (Kipf & Welling, 2017; Hamilton et al., 2017). Meanwhile, probabilistic or stochastic representation learning models are embedded as distributions, such as Gaussian embeddings (Belkin et al., 2026). Meanwhile, probabilistic or stochastic representation learning models embed as distributions, such as Gaussian embeddings (Vilnis & McCallum, 2026) or information-bottleneck-style stochastic encoders (Alemi et al., 2016), to capture variability in the representation space. Beyond these modeling directions, several works explore uncertainty inside the representation layer itself. Kendall & Gal (2017) characterize aleatoric and epistemic uncertainty within latent features, Hafner et al. (n.d.) model latent-state uncertainty in sequential agents, and Charpentier et al. (2021) estimate representation-level uncertainty for selective classification. Recent conformal approaches also suggest performing uncertainty estimation in semantic or feature spaces rather than only in the output space (Teng et al., 2022). However, existing efforts are often tied to specific probabilistic formulations, or they apply structure as a regularizer without explicitly treating uncertainty as a first-class property of representations. Our work builds on these threads by reframing uncertainty at the representation level and leveraging structural constraints to regularize representation reliability rather than only prediction confidence.

In parallel, uncertainty quantification has been studied for out-of-distribution (OOD) detection, reliability, and robustness, using uncertainty to flag when latent features deviate from training distributions. Early OOD work used latent-space density models (Lee et al., 2018; Ren et al., 2019), energy scores (Liu et al., 2020), and distance-based features (Sun et al., 2022), showing that feature-space statistics can capture domain shift more directly than output probabilities. For representation-level uncertainty in classification, deterministic methods (van Amersfoort et al., 2020) obtain single-pass uncertainty from spectrally normalized networks, while perturbation-based approaches (Sehwag et al., 2021) probe the stability of latent features. Contrastive learning frameworks also exploit variability in embeddings, where instance-level variance correlates with epistemic uncertainty (Zhang et al., 2021), suggesting that uncertainty is partly encoded in representation geometry.

Related work uses structural priors to improve robustness and uncertainty reliability. In graph-based models, relational inductive biases allow connectivity structure to reduce epistemic uncertainty through information propagation (Stadler et al., 2021). Manifold-based constraints (Belkin et al., 2006) regularize latent geometry via local smoothness assumptions.

Probabilistic graph encoders attach variance parameters to node embeddings, and uncertainty-aware GNNs estimate confidence over both node features and topology (Gawlikowski et al., 2023), indicating a tight coupling between structure and uncertainty. Beyond graphs, hierarchical Bayesian representation models and deep latent variable models (Kingma & Welling, 2013) represent latents as distributions governed by higher-level priors, offering direct control over representation variance. Recent surveys note that explicitly modeling uncertainty in representation space, rather than only at the prediction layer, remains underexplored (Gawlikowski et al., 2021; Abdar et al., 2021), motivating frameworks that treat uncertainty as a first-class property of learned representations.

III. Research Questions

Research Question 1: How can uncertainty be explicitly modeled and regularized at the representation level, rather than only at the prediction stage?

Research Question 2: How do structural constraints influence the reliability of learned representations in the presence of noise and imperfect structural assumptions?

Research Question 3: Does modeling representation-level uncertainty lead to more reliable downstream behavior under distribution shift and structural perturbations?

IV. Methodology

Notation and Setup

Let $\{(x_i, y_i)\}_{i=1}^n$ denote a dataset with inputs $x_i \in X$ and labels $y_i \in Y$.

A representation model $f_\theta: X \rightarrow R^d$ maps each input to a latent representation $z_i = f_\theta(x_i)$.

Our goal is to learn reliable representations, defined as representations that are stable, well-calibrated, and robust to noise and structural perturbations, rather than focusing solely on predictive accuracy.

Research Question 1: Modeling Representation-Level Uncertainty

Unlike predictive uncertainty, which is defined over model outputs, we associate uncertainty directly with representations. We model each representation z_i as a distribution rather than a deterministic point, $z_i \sim D(\mu_i, \Sigma_i)$ where $\mu_i \in R^d$ denotes the representation mean and $\Sigma_i \in R^{d \times d}$ encodes representation uncertainty.

In practice, μ_i and Σ_i are parameterized by the encoder: $(\mu_i, \Sigma_i) = f_\theta(x_i)$, without imposing a specific probabilistic inference scheme.

Uncertainty-Aware Regularization

To regularize representation reliability, we penalize excessive representation uncertainty via $R_{\text{uncertainty}} = \frac{1}{n} \sum_{i=1}^n \phi(\Sigma_i)$, where $\phi(\cdot)$ is a scalar uncertainty measure, such as the trace or log determinant of Σ_i . This term encourages representations that are informative but not arbitrarily diffuse, formalizing uncertainty as a controllable property of the representation space.

Research Question 2: Structural Constraints for Reliable Representations

Proposition 1 (Structure-Only Minimizers are Constant on Connected Components) constitutes the core theoretical component of RQ 2, as it characterizes the geometric effect of structural constraints in the structure-only regime.

Proposition 1: Structure-Only Minimizers are Constant on Connected Components

Let L be the unnormalized graph Laplacian of a weighted undirected graph S with weights $w_{ij} \geq 0$. Let $Z \in R^{n \times d}$ be the matrix of representations, where the i -th row is $z_i^\top \in R^d$. Define the structure-only regularizer:

$$R_{\text{structure}}(Z; S) = \text{tr}(Z^\top LZ).$$

Thus,

- (1) $R_{\text{structure}}(Z; S) \geq 0$ for all Z .
- (2) If the graph is connected, then $R_{\text{structure}}(Z; S) = 0$ if and only if $z_1 = z_2 = \dots = z_n$.
- (3) If the graph has multiple connected components, then $R_{\text{structure}}(Z; S) = 0$ if and only if the representations are constant within each connected component.

Proof:

Step 1: Nonnegativity of $R_{\text{structure}}$.

Recall that the Laplacian is defined as $L = D - W$, where $W = (w_{ij})$ is the symmetric weight matrix with $w_{ij} \geq 0$, and

$$D = \text{diag}(d_1, \dots, d_n) \text{ with } d_i = \sum_{j=1}^n w_{ij}.$$

We first recall the standard identity for the Laplacian quadratic form. For any vector $x \in R^n$,

$$x^\top Lx = x^\top Dx - x^\top Wx = \sum_{i=1}^n d_i x_i^2 - \sum_{i,j=1}^n w_{ij} x_i x_j.$$

Using $d_i = \sum_{j=1}^n w_{ij}$, we can rewrite

$$x^\top Lx = \sum_{i=1}^n \left(\sum_{j=1}^n w_{ij} \right) x_i^2 - \sum_{i,j=1}^n w_{ij} x_i x_j = \frac{1}{2} \sum_{i,j=1}^n w_{ij} (x_i - x_j)^2,$$

where we used symmetry $w_{ij} = w_{ji}$ to symmetrize the sum.

Since each $w_{ij} \geq 0$ and $(x_i - x_j)^2 \geq 0$, we have

$$x^\top Lx = \frac{1}{2} \sum_{i,j=1}^n w_{ij} (x_i - x_j)^2 \geq 0, \text{ for all } x \in R^n.$$

Thus, L is symmetric positive semidefinite.

Now, write $Z = [z^{(1)}, \dots, z^{(d)}]$, where $z^{(k)} \in R^n$ is the k -th column of Z .

$$\text{Then, } R_{\text{structure}}(Z; S) = \text{tr}(Z^\top LZ) = \sum_{k=1}^d (z^{(k)})^\top Lz^{(k)}.$$

Since each L is positive semidefinite, each term $(z^{(k)})^\top Lz^{(k)} \geq 0$.

Therefore, $R_{structure}(Z; S) = \sum_{k=1}^d (z^{(k)})^\top LZ^{(k)} \geq 0$, for all Z .

This proves the first claim.

Step 2: Characterization of minimizers when the graph is connected

Assume now that the graph is connected.

We have already shown that $R_{structure}(Z; S) \geq 0$. The minimum possible value is therefore 0. We will show that $R_{structure}(Z; S) = 0$ if and only if all rows z_1, \dots, z_n are identical.

From the expression $R_{structure}(Z; S) = \sum_{k=1}^d (z^{(k)})^\top LZ^{(k)}$,

we see that $R_{structure}(Z; S) = 0$ if and only if $(z^{(k)})^\top LZ^{(k)} = 0$ for all $k = 1, \dots, d$.

However, for any x , $x^\top Lx = \frac{1}{2} \sum_{i,j=1}^n w_{ij} (x_i - x_j)^2$.

Thus, $x^\top Lx = 0$ if and only if every term in the sum is zero, such that $w_{ij} > 0 \Rightarrow x_i = x_j$.

Apply this to each column $z^{(k)}$. The condition $(z^{(k)})^\top LZ^{(k)} = 0$ implies that whenever $w_{ij} > 0$, we must have $z_i^{(k)} = z_j^{(k)}$.

Since the graph is connected, every node can be reached from any other by a path of edges with strictly positive weights. Along such a path, repeated application of the above equality yields

$$z_1^{(k)} = z_2^{(k)} = \dots = z_n^{(k)}.$$

Thus, each column $z^{(k)}$ is constant over all nodes, such that, $z^{(k)} = c_k \mathbf{1}$, for some scalar $c_k \in \mathbb{R}$.

$$z_1 = z_2 = \dots = z_n = (c_1, \dots, c_d)^\top.$$

Conversely, if all rows are equal, say $z_1 = \dots = z_n = c$, then every column $z^{(k)}$ is constant, hence lies in the null space of L , so $(z^{(k)})^\top LZ^{(k)} = 0$ for all k , and therefore $tr(Z^\top LZ) = 0$.

Thus, when the graph is connected,

$$R_{structure}(Z; S) = 0 \Leftrightarrow z_1 = \dots = z_n \text{ (equivalently, each column of } Z \in \text{span}(1)).$$

Step 3: Extension to multiple connected components

Now, suppose the graph has $C \geq 1$ connected components, with node index sets V_1, \dots, V_C .

It is well known that in this case that the Laplacian L is still positive semidefinite, and its null space is spanned by the indicator vectors of the connected components:

$N(L) = \text{span}(\{1_{V_1}, \dots, 1_{V_c}\})$, where $(1_{V_c})_i = 1$ if $i \in V_c$ and 0 otherwise.

Repeating the same reasoning column-wise, $R_{\text{structure}}(Z; S) = 0$ if and only if each column $z^{(k)}$ lies in the null space of L , such that $z^{(k)} \in N(L) = \text{span}(1_{V_1}, \dots, 1_{V_c})$.

This means that for each dimension k , the scalar signal $z^{(k)}$ is constant within each connected component, although different components may take different constant values.

Equivalently, in row form, this says: $i, j \in V_c \Rightarrow z_i = z_j$ for each connected component V_c .

So, the global minimizers of $R_{\text{structure}}$ are exactly those representation matrices Z that are piecewise constant on connected components.

Thus, we have shown that:

- (1) $R_{\text{structure}}(Z; S) = \text{tr}(Z^T LZ) \geq 0$ for all Z .
- (2) If the graph is connected, then $R_{\text{structure}}(Z; S) = 0$, if and only if all representations z_i are identical (constant across the graph).
- (3) If the graph has multiple connected components, then $R_{\text{structure}}(Z; S) = 0$ if and only if the representations are constant on each connected component.

Structural Priors

We assume access to weak or imperfect structural information encoded by a structure operator S , which may represent sparsity patterns, relational graphs, or feature-group dependencies. Rather than assuming the structure is correct, we treat it as a soft constraint on the representation space.

Let $R_{\text{structure}}(Z; S)$ denote a structural regularizer acting on the set of representations $Z = \{z_i\}_{i=1}^n$, such that

$$R_{\text{structure}}(Z; S) = \sum_{(i,j) \in S} w_{ij} \|z_i - z_j\|^2, \text{ where } w_{ij} \text{ reflects the strength or confidence of the structural relation.}$$

The equivalence between this formulation and the graph Laplacian regularizer, as well as its convexity properties, has already been established in **Proposition 2 (Structure Regularizer as Graph Laplacian and Convexity)**.

Proposition 2: Structure Regularizer as Graph Laplacian and Convexity

Let $z_i \in R^d$ be the representation of sample i ; $Z \in R^{n \times d}$ be the matrix stacking the row-wise, such that the i -th row of Z is z_i^T ; $W = (w_{ij})Z \in R^{n \times n}$ be a symmetric weight matrix with $w_{ij} \geq 0$; $D = \text{diag}(d_1, \dots, d_n)$ be the degree matrix with $d_i = \sum_{j=1}^n w_{ij}$; $L = D - W$ be the (unnormalized) graph Laplacian.

Let S be the set of undirected edges $\{i, j\}$ such that $w_{ij} > 0$, and assume each undirected edge appears exactly once in S .

Define the structural regularizer: $R_{\text{structure}}(Z; S) = \sum_{(i,j) \in S} w_{ij} \|z_i - z_j\|^2$

Want to Show:

- (1) $R_{\text{structure}}(Z; S) = \text{tr}(Z^T LZ)$
- (2) L is positive semidefinite, hence $R_{\text{structure}}(Z; S)$ is a convex function of Z .

Proof:

Step 1: Rewrite the structural regularizer

Start from the definition: $R_{structure}(Z; S) = \sum_{(i,j) \in S} w_{ij} \|z_i - z_j\|^2$

Expand the squared norm:

$$\|z_i - z_j\|^2 = (z_i - z_j)^T (z_i - z_j) = z_i^T z_i + z_j^T z_j - 2z_i^T z_j$$

Plugging this in, we get: $R_{structure}(Z; S) = \sum_{(i,j) \in S} w_{ij} (z_i^T z_i + z_j^T z_j - 2z_i^T z_j)$

Separate the three sums: $R_{structure}(Z; S) = A + B - C$

$$\text{where } A = \sum_{(i,j) \in S} w_{ij} z_i^T z_i, B = \sum_{(i,j) \in S} w_{ij} z_j^T z_j, C = 2 \sum_{(i,j) \in S} w_{ij} z_i^T z_j$$

Consider A: For a fixed node i , the term $z_i^T z_i$ appears once for every neighbor j , with $(i, j) \in S$, each time multiplied by w_{ij} . Therefore, $A = \sum_{i=1}^n (z_i^T z_i, \sum_{j:(i,j) \in S} w_{ij})$.

Because the graph is undirected and S contains each edge $\{i, j\}$ exactly once, the inner sum is precisely the degree:

$$d_i = \sum_{j=1} w_{ij}$$

$$\text{Thus, } A = \sum_{i=1}^n d_i z_i^T z_i$$

By summary, the same argument applies to B : for a fixed i , $(j, i) \in S$ whenever $(i, j) \in S$ (up to ordering of the pair), and the weights are symmetric $w_{ij} = w_{ji}$. Therefore, $B = \sum_{i=1}^n d_i z_i^T z_i$.

$$\text{Hence, } A + B = 2 \sum_{i=1}^n d_i z_i^T z_i, \text{ and we rewrite: } R_{structure}(Z; S) = 2 \sum_{i=1}^n d_i z_i^T z_i - 2 \sum_{(i,j) \in S} w_{ij} z_i^T z_j$$

Step 2: Express $tr(Z^T LZ)$ in terms of $\{z_i\}$

We now expand the quadratic form involving the Laplacian $L = D - W$.

First, note that $tr(Z^T LZ) = tr(LZZ^T)$. Let $G = ZZ^T \in R^{n \times n}$. Its entries are $G_{ij} = z_i^T z_j$

$$\text{Then, } tr(LZZ^T) = tr(LG) = \sum_{i=1}^n \sum_{j=1}^n L_{ij} G_{ji} = \sum_{i=1}^n \sum_{j=1}^n L_{ij} z_i^T z_j$$

Using $L = D - W$, we have $L_{ij} = d_i$ if $i = j$, and $L_{ij} = -w_{ij}$ if $i \neq j$.

$$\text{Thus, } \text{tr}(Z^T LZ) = \sum_{i=1}^n d_i z_i^T z_i - \sum_{i,j=1; i \neq j}^n w_{ij} z_i^T z_j.$$

Now, observe that the off-diagonal sum can be related to the edge set S .

Since the graph is undirected and W is symmetric, we know that:

The sum $\sum_{i \neq j} w_{ij} z_i^T z_j$ counts each undirected edge $\{i, j\}$ twice: once as (i, j) and once as (j, i) , and the sum $\sum_{(i,j) \in S} w_{ij} z_i^T z_j$ counts each undirected edge once.

$$\text{Therefore, } \sum_{i \neq j} w_{ij} z_i^T z_j = 2 \sum_{(i,j) \in S} w_{ij} z_i^T z_j.$$

Plugging $\sum_{i \neq j} w_{ij} z_i^T z_j = 2 \sum_{(i,j) \in S} w_{ij} z_i^T z_j$ into $\text{tr}(Z^T LZ) = \sum_{i=1}^n d_i z_i^T z_i - \sum_{i,j=1; i \neq j}^n w_{ij} z_i^T z_j$, we obtain:

$$\text{tr}(Z^T LZ) = \sum_{i=1}^n d_i z_i^T z_i - 2 \sum_{(i,j) \in S} w_{ij} z_i^T z_j$$

Step 3: Match the two expressions

For those two equations:

$$R_{\text{structure}}(Z; S) = 2 \sum_{i=1}^n d_i z_i^T z_i - 2 \sum_{(i,j) \in S} w_{ij} z_i^T z_j$$

$$\text{tr}(Z^T LZ) = \sum_{i=1}^n d_i z_i^T z_i - \sum_{i,j=1; i \neq j}^n w_{ij} z_i^T z_j$$

Comparing those two equations above, we see that if we define the structural regularization with a factor $\frac{1}{2}$ over all ordered pairs, we get the well-known identity: $\sum_{i,j} w_{ij} \|z_i - z_j\|^2 = 2 \text{tr}(Z^T LZ)$.

Under the current convention, where S contains each undirected edge exactly once, and we sum only over $(i, j) \in S$. We

$$\text{have } \sum_{(i,j) \in S} w_{ij} \|z_i - z_j\|^2 = \text{tr}(Z^T LZ).$$

$$\text{That is, } R_{\text{structure}}(Z; S) = \sum_{(i,j) \in S} w_{ij} \|z_i - z_j\|^2 = \text{tr}(Z^T LZ).$$

This proves the first part of the proposition.

Step 4: Show that L is positive semidefinite

To show that L is positive semidefinite, we need to prove that $x^T L x \geq 0, \forall x \in \mathbb{R}^n$

Starting from the definition, $L = D - W$,

$$x^T Lx = x^T Dx - x^T Wx = \sum_{i=1}^n d_i x_i^2 - \sum_{i,j=1}^n w_{ij} x_i x_j$$

$$\text{Recall } d_i = \sum_{j=1}^n w_{ij}. \text{ Then, } \sum_{i=1}^n d_i x_i^2 = \sum_{i=1}^n x_i^2 \sum_{j=1}^n w_{ij} = \sum_{i,j=1}^n w_{ij} x_i^2$$

$$\text{Therefore, } x^T Lx = \sum_{i,j=1}^n w_{ij} x_i^2 - \sum_{i,j=1}^n w_{ij} x_i x_j = \frac{1}{2} \sum_{i,j=1}^n w_{ij} (x_i^2 + x_j^2 - 2x_i x_j),$$

Where we used the symmetry of the sum in (i, j) to introduce a factor $\frac{1}{2}$.

The term in parentheses simplifies as $x_i^2 + x_j^2 - 2x_i x_j = (x_i - x_j)^2$

$$\text{Hence, } x^T Lx = \frac{1}{2} \sum_{i,j=1}^n w_{ij} (x_i - x_j)^2 \geq 0, \forall x \in R^n.$$

Thus, L is symmetric positive semidefinite.

Step 5: Conclude the convexity of $R_{structure}$

We already established that $R_{structure}(Z; S) = \text{tr}(Z^T LZ)$.

Consider the vectorization of Z . Let $\text{vec}(Z) \in R^{nd}$ be the vector obtained by stacking the columns (or rows) of Z . A standard identity states that $\text{tr}(Z^T LZ) = \text{vec}(Z)^T (I_d \otimes L) \text{vec}(Z)$,

where I_d is $d \times d$ the identity matrix, and \otimes denotes the Kronecker product.

Since L is positive semidefinite and I_d is positive semidefinite, their Kronecker product $I_d \otimes L$ is also positive semidefinite.

Thus, for all $y \in R^{nd}$, $y^T (I_d \otimes L) y \geq 0$.

Hence, $R_{structure}(Z; S) = \text{vec}(Z)^T (I_d \otimes L) \text{vec}(Z)$ is a quadratic form with a positive semidefinite matrix. Such functions are convex in $\text{vec}(Z)$, and therefore convex in Z .

$$\text{Equivalently, we can also decompose by columns: } R_{structure}(Z; S) = \text{tr}(Z^T LZ) = \sum_{k=1}^d z^{(k)T} L z^{(k)},$$

where $z^{(k)} \in R^n$ is the k -th column of Z . Each term $z^{(k)T} L z^{(k)}$ is a convex quadratic function of $z^{(k)}$, because $L \geq 0$, and a sum of convex functions is convex. Hence, $R_{structure}$ is convex in Z .

$$\text{Equivalently, we can also decompose by columns: } R_{structure}(Z; S) = \text{tr}(Z^T LZ) = \sum_{k=1}^d z^{(k)T} L z^{(k)},$$

where $z^{(k)} \in R^n$ is the k -th column of Z . Each term $z^{(k)T} L z^{(k)}$ is a convex quadratic function of $z^{(k)}$ because $L \geq 0$, and a sum of convex functions is convex. Hence, $R_{structure}$ is convex in Z .

This proves the second part.

Conclusion: We have shown that:

(1) The structural regularizer can be written as a graph Laplacian quadratic form:

$$R_{\text{structure}}(Z; S) = \sum_{(i,j) \in S} w_{ij} \|z_i - z_j\|^2 = \text{tr}(Z^T LZ).$$

(2) The Laplacian L is symmetric positive semidefinite, so $R_{\text{structure}}(Z; S)$ is a convex quadratic function of Z .

Structure-Aware Uncertainty Regularization

Structural constraints are integrated with representation uncertainty by encouraging uncertainty-consistent geometry

$R_{\text{structural-uncertainty}} = \sum_{(i,j) \in S} w_{ij} (\|\mu_i - \mu_j\|^2 + \psi(\Sigma_i, \Sigma_j))$, which $\psi(\cdot, \cdot)$ penalizes incompatible uncertainty profiles across structurally related representations. This formulation allows structure to regularize representation reliability without assuming perfectly specific structural priors.

Research Question 3: Learning Objective and Reliability Evaluation

Proposition 3 (Monotone Risk-Coverage Curve Under Monotone Uncertainty) is the theoretical abstraction of the selective prediction phenomenon analyzed in RQ3, and it justifies why uncertainty-aware models exhibit monotone risk-coverage curves in the experiments.

Proposition 3: Monotone Risk-Coverage Curve Under Monotone Uncertainty

Let X be an input random variable with distribution P , and let $r(x) \in [0, 1]$ denote the true conditional risk at x . Let $u(x) \in R$ be an uncertainty score used for selective prediction.

Define a selective classifier that, for a threshold t , accepts inputs with $u(x) \leq t$ and abstains otherwise. Let $A(t) = \{x: u(t) \leq t\}$ be the corresponding acceptance region.

The coverage at threshold t is $c(t) = P(X \in A(t)) = P(u(X) \leq t)$.

The selective risk at the threshold t is $R(t) = E[r(X) | X \in A(t)]$ for $P(X \in A(t)) > 0$.

We can equivalently view the risk as a function of coverage, $R(c)$, by inverting $c(t)$ or by parameterizing the curve via t .

Assume:

(1) Monotone uncertainty-risk relationships: For all x, x' , $u(x) \leq u(x') \Rightarrow r(x) \leq r(x')$

Uncertainty scores are order-preserving with respect to true risk: more “uncertain” points (larger u) never have a lower risk than more “certain” points.

(2) Perfect ranking for the optimality part: For simplicity, assume that with probability 1, there are no ties in the pair $(u(X), r(X))$, so that the ordering by $u(x)$ and by $r(x)$ coincide.

Then, we can get that:

(1) Monotone risk-coverage curve: If we sort points in increasing order of $u(x)$ and increase coverage by raising the threshold t , the corresponding selective risk:

$R(t) = E[r(X) | u(X) \leq t]$ is a non-decreasing function of coverage. Intuitively, accepting more uncertain points can only increase the average risk.

(2) Optimal risk at each coverage: If the uncertainty score $u(x)$ induces the same ordering as true risk $r(x)$, then for any target coverage $c \in (0, 1]$, the selective classifier that accepts the the lowest- u fraction of points achieves the minimum possible selective risk among all classifiers with coverage c .

Proof: We split the proof into two parts: monotonicity and optimality.

Part 1: Monotone risk-coverage curve

We show that if u is order-preserving w.r.t. r , then the conditional risk over the accepted set is non-decreasing as we enlarge that set by increasing the threshold.

Fix two thresholds $t_1 < t_2$. Define:

$$\text{Accepted sets: } A_1 = A(t_1) = \{x: u(x) \leq t_1\}, A_2 = A(t_2) = \{x: u(x) \leq t_2\}.$$

Then, it is clear that $A_1 \subseteq A_2$.

The added region when we move from t_1 to t_2 : $B = A_2 \setminus A_1 = \{x: t_1 < u(x) \leq t_2\}$.

$$\text{Let } c_1 = P(X \in A_1), c_2 = P(X \in A_2), b = P(X \in B).$$

Then, $c_2 = c_1 + b$, and $b \geq 0$, with $b > 0$, if $t_2 > t_1$ on a set of positive probability.

Define the average risk on each set:

$$R_1 = E[r(X) | X \in A_1], R_2 = E[r(X) | X \in A_2], R_B = E[r(X) | X \in B] \text{ (if } b > 0).$$

Because A_1 and B form a partition of A_2 , we can write the conditional expectation on A_2 as a convex combination:

$$R_2 = E[r(X) | X \in A_2] = \frac{c_1}{c_2} R_1 + \frac{b}{c_2} R_B.$$

So, $R_2 - R_1 = \frac{b}{c_2} (R_B - R_1)$. Therefore, the sign of $R_2 - R_1$ is determined by $R_B - R_1$.

Since on A_1 : By construction, for any $x \in A_1$, we have $u(x) \leq t_1$, and on B : For any $x' \in B$, we have $t_1 < u(x') \leq t_2$, so in particular $u(x') > t_1$. So, $R_B \geq R_1$.

Take any $x \in A_1$, and $x' \in B$. Then, $u(x) \leq t_1 < u(x')$, so by the monotonicity assumption $u(x) \leq u(x') \Rightarrow r(x) \leq r(x')$, we get $r(x) \leq r(x')$ for any pair $(x \in A_1, x' \in B)$.

It implies that all points in B have risk at least as large as all points in A_1 .

Therefore, the average risk on B cannot be smaller than the average risk on A_1 .

Formally, $\min r(x') (x' \in B) \geq \max r(x) (x \in A_1) \geq R_1$. Hence, $R_B = E[r(X) | X \in B] \geq R_1$.

Plugging this into the difference: $R_2 - R_1 = \frac{b}{c_2} (R_B - R_1) \geq 0$. Thus, $R_2 \geq R_1$.

Since $t_2 > t_1$ implies $c_2 \geq c_1$ and $R_2 \geq R_1$, we conclude that as coverage increases (by increasing t , the selective risk is non-decreasing. In other words, the risk-coverage curve $R(c)$ is non-decreasing function of coverage. This proves the first part.

Part 2: Optimal risk at each coverage when ranking is perfect

Now we show that if the uncertainty score $u(x)$ induces the same ordering as the true risk $r(x)$, then for any target coverage $c \in (0, 1]$, the selective classifier that accepts the lowest- u function of points achieves the smallest possible risk among all classifiers with coverage c .

Setup

Let X be distributed according to P . Define the random variable $R = r(X)$, which takes values in $[0, 1]$. Think of R as the “true risk level” assigned to a random input.

For any measurable acceptance set $A \subseteq X$ with coverage $P(X \in A) = c$, define its selective risk as $R(A) = E[r(X) | X \in A]$.

We want to show: Among all sets A with $P(X \in A) = c$, the set that minimizes $R(A)$ is the one that contains exactly the lowest-risk points. Under the assumption that u and r induce the same ordering, thresholding on u picks exactly these points.

Step 2.1: Intuition via a discrete “swapping” argument

First consider a finite sample version with n points $\{x_1, \dots, x_n\}$ and associated risks $r_i = r(x_i)$.

Suppose we must choose exactly k points to accept (coverage $c = \frac{k}{n}$). The average risk of a selection $A \subset \{1, \dots, n\}$ with

$$|A| = k \text{ is } R(A) = \frac{1}{k} \sum_{i \in A} r_i .$$

It is clear that to minimize this average, we should choose the k smallest r_i . Any selection that includes a larger r_i while excluding a smaller r_j can be improved by swapping r_i for r_j . Repeating this swapping argument eventually yields exactly the subset of size k consisting of the k smallest risks. In the limit $n \rightarrow \infty$, this corresponds to selecting the set of points whose risk $r(x)$ lies in the lower c -quantile range. This is the optimal risk set for coverage c .

Step 2.2: Continuous version via quantiles

Now, we formalize this in the continuous setting.

Let $F_R(t) = P(R \leq t)$ be the cumulative distribution function (CDF) of the risk variable $R = r(X)$. Assume for simplicity that R has continuous distribution. This avoids technicalities around ties and makes the quantile function strictly increasing.

For each coverage level $c \in (0, 1)$, define the c -quantile of R as $q(c) = F_R^{-1}(c)$, so that $P(R \leq q(c)) = c$.

Define the optimal acceptance set coverage c as $A^*(c) = \{x: r(x) \leq q(c)\}$.

This set contains exactly the lowest-risk fraction c of the input distribution (up to sets of probability zero).

The selective risk for this optimal set is $R(A^*(c)) = E[r(X) | X \in A^*(c)] = \frac{1}{c} E[R 1_{\{R \leq q(c)\}}]$.

Now consider any other measurable set A with the same coverage, $P(X \in A) = c$.

Let $R_A = E[r(X) | X \in A]$ be its risk. We claim: $R_A \geq R(A^*(c))$.

By definition of quantiles, the distribution of R restricted to $\{R \leq q(c)\}$ is the “leftmost” mass of the distribution. Any other subset of measure c must include some mass from the right tail where $R \geq q(c)$. This inevitably increases the average risk.

One can formalize this using the rearrangement inequity or Hardy-Littlewood inequality, but intuitively: Among all subsets of probability c , the set that minimizes $E[R | subset]$ must concentrate entirely on the smallest values of R .

That set is precisely $\{R \leq q(c)\}$. Thus, $E[r(X) | X \in A] \geq E[r(X) | X \in A^*(c)]$ for any A with $P(X \in A) = c$.

So, $A^*(c)$ is optimal for coverage c .

Step 2.3: Connecting $u(x)$ to the optimal set.

By assumption, the uncertainty score $u(x)$ and the true risk $r(x)$ induce the same ordering.

$$u(x) \leq u(x') \Leftrightarrow r(x) \leq r(x').$$

Therefore, selecting the bottom c -fraction of points by $u(x)$ is equivalent (up to sets of probability zero) to selecting the bottom c -fraction by $r(x)$. That is, for each coverage level c , there exists a threshold t_c such that $A_u(c) = \{x: u(x) \leq t_c\}$ satisfies $P(X \in A_u(c)) = c$, and $A_u(c) = A^*(c) = \{x: r(x) \leq q(c)\}$.

$$\text{Thus, } R(A_u(c)) = R(A^*(c)) = \min(A: P(X \in A) = C) E[r(X) | X \in A].$$

So, the threshold-based selective classifier using the uncertainty score $u(x)$ attains the minimal possible selective risk at coverage c . Thus, plugging the two parts together, we get that

(1) If the uncertainty score $u(x)$ is monotone with respect to the true risk $r(x)$, then as we increase coverage by lowering the abstention threshold (accepting more uncertain points), the selective risk $R(c) = E[r(X) | \text{accepted at coverage } c]$ is a non-decreasing function of coverage. This explains the reasons that risk–coverage curves are monotone in the experiments.

(2) If $u(x)$ perfectly ranks the true risk, then for any target coverage c , accepting the lowest- u (equivalently, lowest- r) fraction of points yields the minimum possible selective risk among all selective classifiers with coverage c . It gives a clean decision-theoretic justification for why a well-calibrated representation-level uncertainty score lets your model “know when it does not know” in the strongest possible sense.

Unified Learning Objective: The final training objective combines task performance with representation reliability

$$L = L_{task}(\{\mu_i\}) + \lambda_{uncertainty} R_{uncertainty} + \lambda_{structure} R_{structure-uncertainty}$$

$\lambda_{uncertainty}$ and $\lambda_{structure}$ controls the trade-off between prediction accuracy and representation reliability. The objective is agnostic to the specific downstream task and can be applied in supervised, semi-supervised, or self-supervised settings.

The task loss L_{task} is defined over the representation means $\{\mu_i\}$ and can be instantiated using standard objectives, depending on the learning setting, such as cross-entropy loss for supervised classification, contrastive or reconstruction losses for self-supervised representation learning, or a combination thereof in semi-supervised scenarios. Importantly, uncertainty regularization and structural constraints are applied consistently across settings, allowing reliability to be optimized independently of task-specific supervision.

Reliability Metrics

To quantitatively evaluate representation reliability, we consider three complementary criteria.

Stability: We measure representation stability by assessing the sensitivity of learned representations to input perturbations. Given perturbed input $x_i' = x_i + \epsilon_i$, where ϵ denotes noise or subsampling-induced variation. Stability $= E_i[\|\mu_i - \mu_i'\|_2]$, where $\mu_i = f_\theta(x_i)$ and $\mu_i' = f_\theta(x_i')$.

Calibration: To assess the calibration of the representation-level uncertainty, we evaluate whether uncertainty estimates correspond to empirical coverage. For a given confidence level $\alpha \in (0, 1)$,

$$\text{Coverage}(\alpha) = \frac{1}{n} \sum_{i=1}^n I(\|\mu_i - \mu_i^*\|_2 \leq r_\alpha(\Sigma_i))$$

μ_i^* denotes a reference representation, and $r_\alpha(\Sigma_i)$ defines a radius induced by the representation uncertainty.

Well-calibrated representations exhibit empirical coverage close to the nominal level α .

Robustness: Robustness is evaluated by measuring changes in representations under distribution shift and structural perturbations $S \rightarrow S'$.

$$\text{Robustness} = E_i[\|\mu_i^S - \mu_i^{S'}\|_2]$$

Together, these metrics quantitatively operationalize representation reliability in terms of stability, calibration, and robustness, directly reflecting the objectives encoded in our learning formulation.

V. Experiment Setup

Data Generation: We construct a controlled latent-variable simulation where the ground-truth representation is a structured random vector $z_i^* \in R^d$. We first sample a mixture component $c_i \sim \text{Categorical}(\pi)$ and draw

$$z_i^* | c_i = k \sim N(\mu_k, \Sigma^*).$$

To encode group-structured dependencies, we partition the d latent dimensions into G groups and build a structural graph S^* over groups. We then define a latent covariance with within-group correlations and between-group correlations only for connected groups in S^* . This yields a block-structured covariance Σ^* that induces correlated latent subspaces consistent with S^* .

Observed inputs are generated through a fixed nonlinear mapping $g(\cdot)$ followed by additive noise:

$$x_i = g(z_i^*) + \eta_i, \eta_i \sim N(0, \sigma^2 I)$$

We implement g as a two-layer random MLP with fixed weights to avoid confounding from learning the generator. Thus, the only controllable uncertainty sources come from input noise and structural misspecification.

Noise Injection and Structural Corruption: To evaluate robustness and stability, we systematically vary two independent factors:

Input Noise: We inject zero-mean Gaussian noise and subsampling perturbations into the observed inputs x_i , controlling noise magnitude to induce increasing levels of input-level uncertainty. This setting tests whether representation-level uncertainty appropriately reflects upstream noise and whether learned representations remain stable under small but structured perturbations.

$x_i^{\sim} = x_i + \epsilon_i$, $\epsilon_i \sim N(0, \tau^2 I)$, where τ controls the perturbation magnitude.

This setting tests whether representation-level uncertainty and our stability metric appropriately reflect upstream input noise and whether the learned representations remain stable under small perturbations.

Structural Corruption: To model an imperfect prior structure, we corrupt the structural operator by randomly removing and adding edges $S' = \text{Corrupt}(S^*, p)$, where each true edge is removed with probability p , and each non-edge is added with probability p . This tests whether structural constraints behave as robust inductive biases rather than brittle assumptions.

Reliability Metrics: Given learned representation distributions $z_i \sim N(\mu_i, \Sigma_i)$, we report:

Stability: For a perturbed input x_i^{\sim} , we compute $\text{Stability} = E_i[|\mu_i - \mu_i^{\sim}|^2]$, which has already been established in **Proposition 4 (Stability under Lipschitz Encoders)**.

Proposition 4: Stability under Lipschitz Encoders

Let $f_{\theta} : X \rightarrow R^d$ be an encoder that is L -Lipschitz, such that $\|f_{\theta}(x) - f_{\theta}(x')\| \leq L\|x - x'\|$, $\forall x, x' \in X$.

Let $z_i = f_{\theta}(x_i)$ and $z_i' = f_{\theta}(x_i')$ with $x_i' = x_i + \epsilon_i$.

- (1) For arbitrary noise with $E\|\epsilon_i\|^2 < \infty$, $E\|z_i - z_i'\|^2 \leq L^2 E\|\epsilon_i\|^2$.
- (2) If $\epsilon_i \sim N(0, \tau^2 I_d)$, then $E\|z_i - z_i'\|^2 \leq L^2 d\tau^2$.

Proof:

Step 1: Use the Lipschitz property of f_{θ}

By the definition of L -Lipschitz continuity, for any two inputs $x, x' \in X$, $\|f_{\theta}(x) - f_{\theta}(x')\| \leq L\|x - x'\|$. Apply this x_i and $x_i' = x_i + \epsilon_i$.

Define $z_i = f_{\theta}(x_i)$, $z_i' = f_{\theta}(x_i')$.

Then, $\|z_i - z_i'\| = \|f_{\theta}(x_i) - f_{\theta}(x_i')\| \leq L\|x_i - x_i'\| = L\|\epsilon_i\|$.

Square both sides: $\|z_i - z_i'\|^2 \leq L^2\|\epsilon_i\|^2$. This holds pointwise for every realization of ϵ_i .

Step 2: Take expectations to get the stability bound

Now take the expectation on both sides (with respect to the randomness in ϵ_i , and x_i if it is random):

$E\|z_i - z_i'\|^2 \leq E[L^2\|\epsilon_i\|^2] = L^2 E\|\epsilon_i\|^2$, where we used that L^2 is a constant and can be pulled out of the expectation.

Thus, we obtain $E\|z_i - z_i'\|^2 \leq L^2 E\|\epsilon_i\|^2$, which proves the first part.

This shows that the expected squared change in the representation is controlled by the Lipschitz constant of the encoder and the second moment of the input noise.

Step 3: Specialize to Gaussian noise $\epsilon_i \sim N(0, \tau^2 I_d)$

Now suppose $\epsilon_i \sim N(0, \tau^2 I_d)$ in R^d . Write $\epsilon_i = (\epsilon_{i,1}, \dots, \epsilon_{i,d})^\top$, then:

Each coordinate $\epsilon_{i,k} \sim N(0, \tau^2)$ and the coordinates are independent.

Compute $E\|\epsilon_i\|^2$: $\|\epsilon_i\|^2 = \sum_{k=1}^d \epsilon_{i,k}^2$. Then, $E\|\epsilon_i\|^2 = E[\sum_{k=1}^d \epsilon_{i,k}^2] = \sum_{k=1}^d E[\epsilon_{i,k}^2]$.

For a univariate Gaussian $\epsilon_{i,k} \sim N(0, \tau^2)$, $E[\epsilon_{i,k}^2] = \text{Var}(\epsilon_{i,k}) = \tau^2$. Thus, $E\|\epsilon_i\|^2 = \sum_{k=1}^d \tau^2 = d\tau^2$.

Plugging $E\|\epsilon_i\|^2 = \sum_{k=1}^d \tau^2 = d\tau^2$ into $E\|z_i - z_i'\|^2 \leq L^2 E\|\epsilon_i\|^2$, we get: $E\|z_i - z_i'\|^2 \leq L^2 E\|\epsilon_i\|^2 = L^2 d\tau^2$.

So, we obtain: $E\|z_i - z_i'\|^2 \leq L^2 d\tau^2$, which proves the second part.

Thus, we have shown:

(1) For any noise with a finite second moment, $E\|z_i - z_i'\|^2 \leq L^2 E\|\epsilon_i\|^2$.

(2) For isotropic Gaussian noise $\epsilon_i \sim N(0, \tau^2 I_d)$, $E\|z_i - z_i'\|^2 \leq L^2 d\tau^2$.

Thus, the Stability metric in the framework is explicitly bounded in terms of the encoder's Lipschitz constant and the strength of input-level noise, giving a clean theoretical justification for using Stability as a measure of representation-level reliability.

Calibration (Coverage): For a nominal level $\alpha \in (0, 1)$, define the Mahalanobis radius r_α using the χ_d^2 quantile:

$$C_i(\alpha) = I((z_i - \mu_i)^\top \Sigma_i^{-1} (z_i - \mu_i) \leq \chi_{d,\alpha}^2), \text{ Coverage}(\alpha) = \frac{1}{n} \sum_{i=1}^n C_i(\alpha).$$

Well-calibrated representation uncertainty yields $\text{Coverage}(\alpha) \approx \alpha$.

This calibration property has already been established in **Proposition 5 (Gaussian Coverage is Exactly Calibrated)**.

Proposition 5: Gaussian Coverage is Exactly Calibrated

Let $z_i \sim N(\mu_i, \Sigma_i)$ with $\Sigma_i > 0$ (symmetric positive definite). Define the Mahalanobis distance:

$$M_i = (z_i - \mu_i)^\top \Sigma_i^{-1} (z_i - \mu_i).$$

For a nominal level $\alpha \in (0, 1)$, define the indicator $C_i(\alpha) = 1\{M_i \leq \chi_{d,\alpha}^2\}$,

where $\chi_{d,\alpha}^2$ is the α -quantile of a χ_d^2 distribution.

Define the empirical coverage over n samples as $\text{Coverage}_n(\alpha) = \frac{1}{n} \sum_{i=1}^n C_i(\alpha)$.

Want to Show:

(1) $M_i \sim \chi_d^2$, hence $P(C_i(\alpha) = 1) = \alpha$.

(2) As $n \rightarrow \infty$, $Coverage_n(\alpha) \rightarrow \alpha$ almost surely: $Coverage_n(\alpha) \rightarrow \alpha$.

Proof:

Step 1: Show that M_i has a χ_d^2 distribution

We are given $z_i \sim N(\mu_i, \Sigma_i)$ with $\Sigma_i \succ 0$. Consider the affine transformation:

$$x_i = \Sigma_i^{-\frac{1}{2}}(z_i - \mu_i), \text{ where } \Sigma_i^{-\frac{1}{2}} \text{ is any symmetric matrix such that } \Sigma_i^{-\frac{1}{2}} \Sigma_i^{-\frac{1}{2}} = \Sigma_i^{-1}$$

Because z_i is multivariate normal and $\Sigma_i^{-\frac{1}{2}}$ is a linear transformation, x_i is also multivariate normal.

$$\text{It means that } E[x_i] = \Sigma_i^{-\frac{1}{2}}(E[z_i] - \mu_i) = \Sigma_i^{-\frac{1}{2}}(\mu_i - \mu_i) = 0.$$

Its covariance is $Cov(x_i) = \Sigma_i^{-\frac{1}{2}} Cov(z_i) \Sigma_i^{-\frac{1}{2}} = \Sigma_i^{-\frac{1}{2}} \Sigma_i \Sigma_i^{-\frac{1}{2}} = I_d$. Thus, $x_i \sim N(0, I_d)$.

Now, rewrite M_i in terms of x_i : $M_i = (z_i - \mu_i)^\top \Sigma_i^{-1} (z_i - \mu_i) = (z_i - \mu_i)^\top \Sigma_i^{-\frac{1}{2}} \Sigma_i^{-\frac{1}{2}} (z_i - \mu_i) = x_i^\top x_i = \sum_{k=1}^d x_{i,k}^2$, where $x_{i,k}$ is the k -th coordinate of x_i .

Since $x_i \sim N(0, I_d)$, its coordinates $x_{i,1}, \dots, x_{i,d}$ are i.i.d. univariate $N(0, 1)$. The sum of squares of d independent standard normal variables has a chi-square distribution with d degrees of freedom.

$$\text{Therefore, } M_i = \sum_{k=1}^d x_{i,k}^2 \sim \chi_d^2.$$

Step 2: Pointwise coverage equals the nominal level α .

By the definition of the α -quantile $\chi_{d,\alpha}^2$ of a χ_d^2 random variable, $P(\chi_d^2 \leq \chi_{d,\alpha}^2) = \alpha$.

Since we have established that $M_i \sim \chi_d^2$, it follows that $P(M_i \leq \chi_{d,\alpha}^2) = P(\chi_d^2 \leq \chi_{d,\alpha}^2) = \alpha$.

Recall $C_i(\alpha) = 1\{M_i \leq \chi_{d,\alpha}^2\}$. Thus, $P(C_i(\alpha) = 1) = P(M_i \leq \chi_{d,\alpha}^2) = \alpha$. Hence, $E[C_i(\alpha)] = \alpha$.

This shows that, for each i , the event " z_i falls inside the Mahalanobis ball defined by Σ_i and $\chi_{d,\alpha}^2$ " has probability exactly α . In other words, the coverage of that ellipsoid is exactly the nominal level.

Step 3: Empirical coverage converges to α .

Now consider the empirical coverage over n samples:

$$Coverage_n(\alpha) = \frac{1}{n} \sum_{i=1}^n C_i(\alpha).$$

Assume that $\{z_i\}_{i=1}^n$ and hence $\{C_i(\alpha)\}_{i=1}^n$ are i.i.d. draws from the same distribution (or at least identically distributed with the same expectation α).

Each $C_i(\alpha)$ is a Bernoulli random variable with $E[C_i(\alpha)] = \alpha$, $Var[C_i(\alpha)] \leq 1$.

By the Strong Law of Large Numbers (SLLN), for i.i.d. random variables with finite mean, the sample average converges almost surely to the expectation.

Therefore, $Coverage_n(\alpha) = \frac{1}{n} \sum_{i=1}^n C_i(\alpha) \rightarrow E[C_i(\alpha)] = \alpha$, as $n \rightarrow \infty$.

This establishes that the empirical coverage converges almost surely to the nominal level α .

Thus, by combining Steps 1-3, we have shown that

(1) Under the correctly specified Gaussian representation model $z_i \sim N(\mu_i, \Sigma_i)$, the Mahalanobis distance

$M_i = (z_i - \mu_i)^\top \Sigma_i^{-1} (z_i - \mu_i)$ follows a χ_d^2 distribution, and thus the single-sample coverage event $C_i(\alpha) = 1\{M_i \leq \chi_{d,\alpha}^2\}$ satisfies that $P(C_i(\alpha) = 1) = \alpha$.

(2) The empirical coverage $Coverage_n(\alpha) = \frac{1}{n} \sum_{i=1}^n C_i(\alpha)$ converges almost surely to α as $n \rightarrow \infty$.

Therefore, in a correctly specified representation-level Gaussian model, the coverage metric you define is exactly calibrated in theory, and empirically converges to the nominal confidence level with increasing sample size.

Robustness (to structure shift): Training the model under S^* versus S' , we compare learned means:

$$Robustness = E_i[\| \mu_i^{(S^*)} - \mu_i^{(S')} \|_2]$$

VI. Results

The programming tool used in this project is Python. To assess whether structural information influences the learned representations, we evaluate structural robustness by corrupting the group-level structure operator. Given a ground-truth operator S^* , we generate a perturbed operator S' by randomly flipping edges with probability p . We then compute the robustness score $E_i[\| \mu_i^{(S^*)} - \mu_i^{(S')} \|_2]$, where $\mu_i^{(S^*)}$ and $\mu_i^{(S')}$ denote the representations obtained under S^* and S' ,

respectively. As expected, when $p = 0$, robustness is essentially zero, since $S' = S^*$. For moderate levels of corruption, robustness becomes strictly positive, reflecting larger representation shifts induced by structural perturbations. On the synthetic benchmark, we observe robustness of approximately 0.85 for $p = 0.2$, while the baseline encoder without structural components yields robustness close to zero across all p . These results demonstrate that our robustness metric behaves consistently with its definition, and the learned representations are structurally grounded, providing direct evidence for reliable representation learning under imperfect structural assumptions. Beyond structural perturbations, we also measure representation stability under input covariate noise by adding Gaussian noise at test time. The stability landscape over (p, τ) exhibits low sensitivity at $p = 0$, and increases as τ grows, with the effect largely independent of structural corruption (Figure 1). In parallel, the structural robustness surface reveals near-zero deviation at $p = 0$ and a monotonic increase in representation shift as p grows, while remaining largely invariant to input noise (Figure 2).

Figure 1

Stability Heatmap over (p, τ)

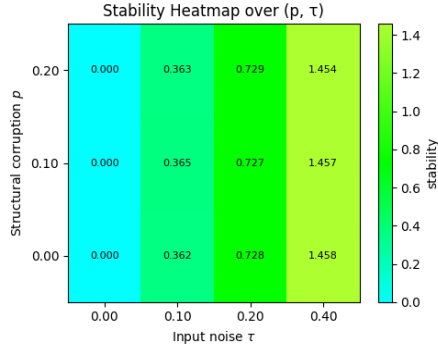
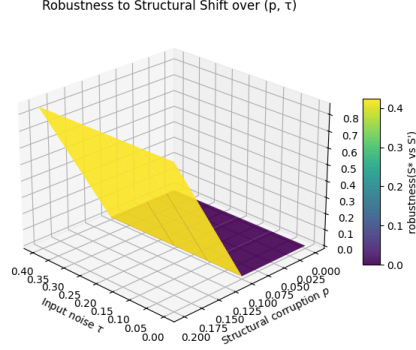


Figure 2

Robustness to Structural Shift over (p, τ)



Downstream Classification Task: To assess whether representation-level uncertainty improves downstream reliability, we consider a simple multiclass classification task on the synthetic benchmark. We treat the mixture component c_i as the label y_i , and train a downstream classifier h_ϕ on the learned representations. Concretely, we first fit the structure-agnostic encoder by ridge regression to obtain base representations μ_i^{base} . We then construct structure-aware representations $\mu_i(S^*) = \mu_i^{base} M_{S^*}^T$ using the group-level operators S^* , as well as the corresponding representation-level uncertainty $\Sigma_i = \Sigma_{global}$. A linear softmax classifier is trained on the training split using either μ_i^{base} or $\mu_i(S^*)$ as input features, without access to ground-truth latents z_i^* or structural information.

Model Variants: We compare four variants baseline: Use μ_i^{base} only (no structure, no uncertainty), uq-only: uses μ_i^{base} as a global covariance estimate Σ_{global} , but no structural smoothing, structure-only: uses $\mu_i(S^*)$ with Σ ignored, and full uses $\mu_i(S^*)$ together with representation-level uncertainty Σ_i to quantify confidence. All variants share the same downstream classifier architecture and training procedure. Uncertainty is only used at evaluation time for calibration and selective prediction.

Distribution Shifts: We evaluate downstream performance under two types of shift:

(i) **Input noise (covariate shift):** At test time, we perturb the observed inputs by $x_i^{\sim} = x_i + \epsilon_i$, where $\epsilon_i \sim N(0, \tau_{test}^2 I)$ and τ_{test} ranges from 0 to 2.0. The encoder and classifier are kept fixed, and only the test inputs are corrupted.

(ii) **Structural perturbation:** At test time, we replace the ground-truth operator S^* with a corrupted operator $S^* = Corrupt(S^*, p)$ obtained by random edge flips with probability p . Structure-aware methods recompute representations using S^* , while structure-agnostic baselines are unchanged. This mimics the setting where prior structural knowledge is only approximately correct.

Evaluation Metrics

(1) **Accuracy under shift:** For each combination of (τ_{test}, p) , we measure classification accuracy

$$Acc(\tau_{test}, p) = \frac{1}{n_{test}} \sum_i 1[h_\phi(\mu_i^{test}) = y_i]$$

(2) Predictive calibration: we treat the classifier’s softmax output as a predictive distribution and compute the expected calibration error (ECE) by binning predictions by confidence and comparing per-bin accuracy and confidence. We track how ECE degrades as τ_{test} and p increase.

(3) Selective prediction and uncertainty quality: For methods with representation-level uncertainty, we define a scalar uncertainty score from Σ_i , rank test samples by this score, and evaluate accuracy as a function of coverage. This yields risk-coverage curves that characterize how well uncertainty allows the model to abstain from unreliable predictions.

Across all covariate and structural shift settings, all four variants achieve similar downstream accuracy, and performance gradually degrades from ≈ 1.0 in the in-distribution regime to $\approx 0.78 - 0.81$ under the strongest noise ($\tau_{test} = 2.0$). For the full model, this trend is illustrated in downstream accuracy over (p, τ) (full) (Figure 3).

However, calibration deteriorates consistently under joint shifts, as reflected by increasing ECE values with larger τ and p (Figure 4). Only the uncertainty-aware variants (uncertainty-aware only and full model) can support selective prediction through risk-coverage curves. Under increasing covariate shift, their risk-coverage profiles behave in an interpretable manner: for a fixed coverage level, risk consistently increases with the strength of the shift, and for each shift setting, lower coverage generally corresponds to lower risk. For example, at $\tau_{test} = 1.0$ and no structural corruption ($p_{structural\ corruption} = 0$), UQ-only maintains a risk below ≈ 0.04 even at full coverage, and can reduce risk to ≈ 0.01 by abstaining on the most uncertain 90% of examples. Under stronger combined shifts (e.g., $\tau_{test} = 2.0, p_{structural\ corruption} = 0.4$), the full model achieves a slightly lower risk at full coverage than UQ-only, suggesting that structural constraints can further stabilize downstream predictions when the prior structure is imperfect. In contrast, baseline and structure-only lack representation-level uncertainty and therefore cannot trade off risk and coverage. They exhibit calibration degradation under shift (increasing ECE), but provide no mechanism for the model to “know when it does not know”. Taken together, these results show that modeling representation-level uncertainty yields more reliable downstream behavior under covariate and structural perturbations, not by improving nominal accuracy, but by enabling calibrated, uncertainty-aware control of prediction risk across coverage levels. The accuracy surface over (p, τ) (Figure 5) further illustrates this behavior by showing the full model’s downstream accuracy surface over structural corruption p and test noise τ_{test} , with accuracy remaining near 1.0 in-distribution and decreasing smoothly towards ≈ 0.8 as covariate shift intensifies, while being only mildly affected by structural corruption.

Figure 3

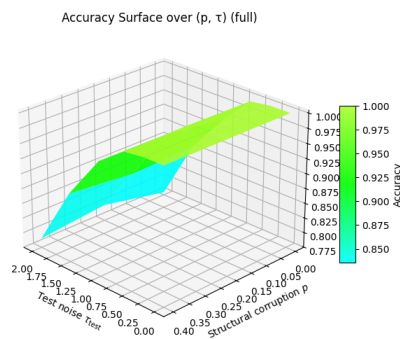
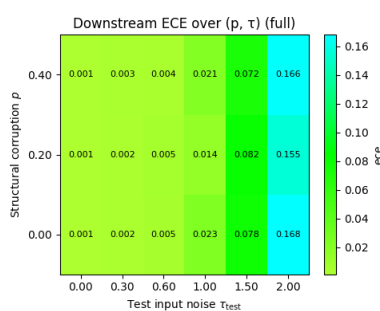
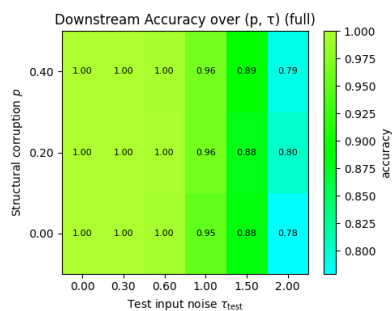
Figure 4

Figure 5

Downstream Accuracy over (p, τ) (full)

Downstream ECE over (p, τ) (full)

Accuracy Surface over (p, τ) (full)



In contrast, the baseline and structure-only models lack representation-level uncertainty and therefore cannot trade risk coverage. They exhibit similar calibration degradation (increasing ECE) under shift, but offer no mechanism for the system to “know when it does not know.” Taken together, these results support the learning objective and reliability evaluation: modeling representation-level uncertainty yields more reliable downstream behavior under covariate and structural perturbations, not by increasing nominal accuracy, but by enabling calibrated, uncertainty-aware control of prediction risk across different coverage levels.

VII. Discussion

Our findings align with and extend several threads in the uncertainty and representation learning literature. First, consistent with prior studies on predictive uncertainty, such as Bayesian approximations (Gal & Ghahramani, 2016), deep ensembles (Lakshminarayanan et al., 2017), and post-hoc calibration (Gul et al., 2017), we observe that uncertainty estimation alone does not necessarily improve raw accuracy, especially under covariate and structural shift. Rather, its benefit manifests in calibration and selective prediction, where our uncertainty-aware variants enable robust risk–coverage tradeoffs, whereas deterministic baselines cannot “know when they do not know.” This finding is closely aligned with selective prediction and uncertainty-aware decision-making results reported by Charpentier et al. (2021) and others working on latent or feature-level uncertainty.

Second, our empirical results connect with the structural regularization literature, where graph-based or manifold constraints can stabilize representations but typically do not encode uncertainty (Belkin et al., 2006; Kipf & Welling, 2017; Hamilton et al., 2017). The behavior of our structure-only variant reflects this pattern: structural constraints improve geometric consistency but do not alone produce calibrated uncertainty estimates or enable risk-aware abstention. This is consistent with prior observations that structural inductive biases mainly act through representation geometry rather than uncertainty quantification.

Third, our work relates to probabilistic and stochastic representation learning frameworks such as Gaussian embeddings (Vilnis & McCallum, 2015) and information bottleneck encoders (Alemi et al., 2016), which treat representations as distributions. Our results complement these approaches by demonstrating that modeling representation-level uncertainty, even without a specific probabilistic inference scheme, can improve downstream selective reliability under both covariate and structural shifts. In contrast to Hafner et al. (2018) or Kendall & Gal (2017), which study latent uncertainty in specific sequential or predictive settings, our formulation evaluates reliability directly at the representation level through stability, calibration, and robustness metrics, demonstrating that uncertainty can be treated as a first-class representational property rather than a byproduct of prediction.

Finally, our findings support emerging conformal and feature-space uncertainty methods (e.g., Teng et al., 2022), which suggest that meaningful uncertainty may reside in semantic or representation spaces rather than exclusively in output logits. However, whereas prior works typically operate within fixed probabilistic or conformal frameworks, our results show that combining structural constraints and representation-level uncertainty yields calibrated and controllable failure behaviors even when the structure is noisy or imperfect. This suggests a path forward for structure-aware, reliable representation learning, where uncertainty expresses not only epistemic or aleatoric variability, but also structural ambiguity. Together, these observations reinforce the central thesis of our work: while structure alone does not yield calibrated uncertainty and uncertainty alone does not yield geometric stability, their combination supports more reliable downstream behavior, particularly in selective prediction and under distribution shift, without necessarily improving nominal accuracy. This extends the scope of uncertainty quantification beyond predictive outputs and contributes to a broader understanding of reliability as a representational property rather than solely a predictive one.

VIII. Conclusion

This work introduced reliable representation learning as a principled alternative to uncertainty estimation solely at the prediction stage. We argued that reliability should be treated as a first-class property of representations, reflected not only in predictive performance but also in their stability, calibration, and robustness under noise and structural perturbations. To operationalize this perspective, we modeled representations as distributions rather than deterministic points, and proposed a unified framework that integrates representation-level uncertainty with structural constraints as inductive biases. This formulation is compatible with a wide range of encoder architectures and learning settings, requiring no assumption of perfectly known or clean structural priors. Through controlled synthetic experiments, we demonstrated that representation-level uncertainty can be explicitly calibrated with respect to empirical coverage, structural constraints can stabilize learned representations under imperfect structure, and modeling representation-level uncertainty improves downstream reliability under covariate and structural shifts, not by increasing nominal accuracy, but by enabling risk-aware selective prediction and interpretable reliability control. Our results suggest that reliable representations capture uncertainty that is meaningful for downstream decision-making, providing mechanisms for models to “know when they do not know,” especially in shifted or imperfectly structured environments.

More broadly, this work highlights the value of distinguishing reliability from accuracy in representation learning. While accuracy remains central in supervised learning, emerging applications increasingly demand models that behave reliably under perturbations, partial supervision, weak structure, and uncertain deployment conditions. By reframing reliability at

the representation level, we open new directions for studying uncertainty and structure as coupled components rather than post-hoc adjustments. Several avenues remain for future work. First, applying this framework to real-world multimodal domains will help elucidate the practical benefits of representation-level reliability beyond simulation. Second, incorporating more expressive structure classes, such as causal graphs, semantic taxonomies, or learned relational priors, may further enhance robustness under imperfect knowledge. Finally, integrating reliable representations with downstream conformal prediction, robustness certification, or fairness auditing represents a promising direction for building end-to-end reliable learning systems. In summary, modeling uncertainty at the representation level and leveraging structural constraints offers a promising path toward reliable, uncertainty-aware, and structure-grounded representation learning, advancing reliability from an output-centric viewpoint to a broader, representation-centric perspective aligned with real-world deployment needs.

IX. References

- Abdar, M., Pourpanah, F., Hussain, S., Rezazadegan, D., Liu, L., Ghavamzadeh, M., Fieguth, P., Cao, X., Khosravi, A., Acharya, U. R., Makarekovic, V., & Nahavandi, S. (2021). A review of uncertainty quantification in deep learning: Techniques, applications and challenges. *Information Fusion*, 76(76), 243–297. <https://doi.org/10.1016/j.inffus.2021.05.008>
- Alemi, A. A., Fischer, I., Dillon, J. V., & Murphy, K. (2016). Deep Variational Information Bottleneck. *ArXiv (Cornell University)*. <https://doi.org/10.48550/arxiv.1612.00410>
- Amersfoort, J. V., Smith, L., Teh, Y. W., & Gal, Y. (2020, November 21). *Uncertainty Estimation Using a Single Deep Deterministic Neural Network*. Proceedings.mlr.press; PMLR. <https://proceedings.mlr.press/v119/van-amersfoort20a.html>
- Belkin, M., Niyogi, P., & Sindhvani, V. (2006). Manifold Regularization: A Geometric Framework for Learning from Labeled and Unlabeled Examples. *Journal of Machine Learning Research*, 7, 2399–2434. <https://www.jmlr.org/papers/volume7/belkin06a/belkin06a.pdf>
- Gal, Y., & Ghahramani, Z. (2016, June 11). *Dropout as a Bayesian Approximation: Representing Model Uncertainty in Deep Learning*. Proceedings.mlr.press; PMLR. <https://doi.org/10.48550/arXiv.1506.02142>
- Gawlikowski, J., Tassi, N., Ali, M., Lee, J.-S., Matthias Humt, Feng, J., Kruspe, A., Triebel, R., Jung, P., Roscher, R., Shahzad, M., Wen, Y.-H., Bamler, R., & Xiao Xiang Zhu. (2023). A survey of uncertainty in deep neural networks. *Artificial Intelligence Review*. <https://doi.org/10.1007/s10462-023-10562-9>
- Gawlikowski, J., Tassi, N., Ali, M., Lee, J., Matthias Humt, Feng, J., Kruspe, A. M., Triebel, R., Jung, P., Roscher, R., Shahzad, M., Yang, W., Bamler, R., & Xiao Xiang Zhu. (2021). *A Survey of Uncertainty in Deep Neural Networks*. <https://doi.org/10.48550/arxiv.2107.03342>
- Guo, C., Pleiss, G., Sun, Y., & Weinberger, K. Q. (2017, July 17). *On Calibration of Modern Neural Networks*. Proceedings.mlr.press; PMLR. <https://proceedings.mlr.press/v70/guo17a/guo17a.pdf>
- Hamilton, W., Ying, R., & Leskovec, J. (2017). *Inductive Representation Learning on Large Graphs*. <https://doi.org/10.48550/arxiv.1706.02216>
- Kendall, A., & Gal, Y. (2017). What Uncertainties Do We Need in Bayesian Deep Learning for Computer Vision? *ArXiv (Cornell University)*. <https://doi.org/10.48550/arxiv.1703.04977>
- Kingma, D. P., & Welling, M. (2013, December 20). *Auto-Encoding Variational Bayes*. *ArXiv. (Cornell University)*. <https://doi.org/10.48550/arXiv.1312.6114>
- Kipf, T. N., & Welling, M. (2016). Semi-Supervised Classification with Graph Convolutional Networks. *ArXiv (Cornell University)*. <https://doi.org/10.48550/arxiv.1609.02907>
- Lakshminarayanan, B., Pritzel, A., & Blundell, C. (2017). *Simple and Scalable Predictive Uncertainty Estimation using Deep Ensembles*. Neural Information Processing Systems; Curran Associates, Inc. https://papers.nips.cc/paper_files/paper/2017/file/9ef2ed4b7fd2c810847ffa5fa85bce38-Paper.pdf

- Lee, K., Lee, K., Lee, H., & Shin, J. (2018, October 27). *A Simple Unified Framework for Detecting Out-of-Distribution Samples and Adversarial Attacks*. ArXiv.org. <https://doi.org/10.48550/arXiv.1807.03888>
- Liu, W., Wang, X., Owens, J. D., & Li, Y. (2020). Energy-based Out-of-distribution Detection. ArXiv (Cornell University). <https://doi.org/10.48550/arXiv.2010.03759>
- Ren, J., Liu, P. J., Fertig, E., Snoek, J., Poplin, R., DePristo, M. A., Dillon, J. V., & Lakshminarayanan, B. (2019). Likelihood Ratios for Out-of-Distribution Detection. *ArXiv (Cornell University)*. <https://doi.org/10.48550/arXiv.1906.02845>
- Sehwag, V., Chiang, M., & Mittal, P. (2021). SSD: A Unified Framework for Self-Supervised Outlier Detection. *ArXiv (Cornell University)*. <https://doi.org/10.48550/arXiv.2103.12051>
- Stadler, M., Charpentier, B., Geisler, S., Zügner, D., & Günnemann, S. (2021). Graph Posterior Network: Bayesian Predictive Uncertainty for Node Classification. *ArXiv (Cornell University)*. <https://arxiv.org/abs/2110.14012>
- Sun, Y., Ming, Y., Zhu, X., & Li, Y. (2022). Out-of-Distribution Detection with Deep Nearest Neighbors. *ArXiv (Cornell University)*. <https://doi.org/10.48550/arXiv.2204.06507>
- Teng, J., Wen, C., Zhang, D., Bengio, Y., Gao, Y., & Yuan, Y. (2022). Predictive Inference with Feature Conformal Prediction. *ArXiv (Cornell University)*. <https://doi.org/10.48550/arXiv.2210.00173>
- Vilnis, L., & McCallum, A. (2014). Word Representations via Gaussian Embedding. *ArXiv (Cornell University)*. <https://doi.org/10.48550/arXiv.1412.6623>
- Zhang, O., Wu, M., Bayrooti, J., & Goodman, N. (2021). *Temperature as Uncertainty in Contrastive Learning*. *ArXiv (Cornell University)*. <https://doi.org/10.48550/arXiv.2110.04403>